Article Beitr. Phys. Atmosph., August 1989, p.165–171
0005-8173/89/03 0165–07 $ 3.00/0 Vol. 62, No. 3 165

# Optical Properties of Clouds Derived from Fully Cloudy AVHRR Pixels

K. T. Kriebel[1], R. W. Saunders[2] and G. Gesell[3]

[1]DLR-Institut für Physik der Atmosphäre, D-8031 Oberpfaffenhofen, FRG

[2]Meteorological Office Unit, Robert-Hooke Institute for Cooperative Atmospheric Research, Clarendon Laboratory, Oxford, UK

[3]DLR-Hauptabteilung Angewandte Datentechnik, D-8031 Oberpfaffenhofen, FRG

(Manuscript received March 1989; in revised form July 1989)

**Abstract**

Based on a reliable identification of cloud-filled AVHRR pixels, known parametrizations of the cloud micro-physics are used to connect cloud optical properties with cloud reflectance. The latter is derived from the measured radiances of the combined earth-atmosphere-cloud system. First validations of the stratus liquid water path and the cirrus optical depth by means of airborne in-situ measurements show agreement to within the expected range of uncertainty of about ± 50%. However, more validations have to be performed before the accuracy of these satellite methods can be firmly established.

**Zusammenfassung**

**Optische Eigenschaften von Wolken, abgeleitet aus vollständig bewölkten AVHRR-Bildelementen**

Basierend auf einer zuverlässigen Identifikation von total bewölkten AVHRR-Pixeln werden bekannte Parametrisierungen der Wolkenmikrophysik verwendet, um optische Eigenschaften von Wolken mit dem Wolkenreflexionsgrad zu verknüpfen. Letzterer wird abgeleitet aus der gemessenen Strahldichte des kombinierten Systems Erde-Atmosphäre-Wolke. Erste Validierungen des Flüssigwasserweges von Stratus und der optischen Dicke von Cirrus durch Flugzeugmessungen stimmen innerhalb des erwarteten Unsicherheitsbereichs von etwa ± 50% überein. Es müssen jedoch noch weitere Validierungen durchgeführt werden, bevor die Genauigkeit dieser Satellitenmethoden festgelegt werden kann.

## 1 Introduction

The optical properties of clouds like optical thickness and liquid or ice water path as derived from satellite data are possibly useful parameters to help validate and initialize general circulation models and limited area models of various scales. Due to improving horizontal resolution of the models, grid mesh cloudiness can be compared with satellite data, as well as optical depth and liquid or ice water path. First attempts have already been made. Sundqvist et al. (1988) use the cloud water as a prognostic variable in a mesoscale NWP model. There are several approaches to relate cloud optical properties with satellite measured radiances (e.g. Arking and Childs, 1985; Rossow et al., 1985; Platt et al., 1980; Stephens, 1978, and Starr and Cox, 1985). Using the 'AVHRR Processing scheme Over cLoud, Land and Ocean' (APOLLO) (Saunders, 1986; Saunders and Kriebel, 1988) which identifies cloud filled pixels, one can make use of parametrized schemes which relate cloud top reflectance to optical properties. We have adopted the parametrization scheme from Stephens (1978) and Stephens et al. (1984). This scheme uses a two-stream approximation of the equation of radiative transfer obtained for optically thin layers in the atmosphere developed by Coakley and Chylek (1975). It relates the cloud reflectance to the optical thickness in a simple formula which depends on only one additional variable, the backscattering coefficient. Stephens has modified the values of the backscattering coefficient to extend the applicability of this formula to water clouds with optical thicknesses up to 500. He has further shown that the optical thickness is mainly due to the liquid water path, if the drop size distribution which is a function of the liquid water path is taken into account by the various cloud models used by Stephens. He deduces simple relations between the optical thickness and the liquid water path and between the liquid water path and the upward and downward infrared emissivities. These parametrizations will apply under normal atmospheric conditions. In extreme conditions, like heavily polluted air, the relationships may have errors which exceed the ± 10 per cent given by Stephens. For ice clouds we use a relation between cloud reflectance and optical thickness given by Platt et al. (1980)

and a relation between the cloud reflectance and the infrared emissivity and the ice water path given by Starr and Cox (1985).

All these parametrizations make use of the directional hemispherical reflectance of the cloud because this quantity expresses the microphysical state of the cloud in terms of upwelling radiant energy flux density, divided by the solar irradiance. However, this quantity is not directly obtained from measurements. The observable quantity is the bidirectional reflectance factor of the earth-atmosphere-cloud system at the top of the atmosphere (for nomenclature see Nicodemus, 1970, and Kriebel and Koepke, 1987). Firstly, the relationship of both reflection quantities is described. Secondly, the parametrization formulae used are given and finally first validations are presented and discussed.

## 2 Determination of Cloud Reflectance

Satellite instruments like the NOAA AVHRR receive an upwelling radiance determined by the instrument's field-of-view and spectral passband. After calibrating the instrument (e.g. Kidwell, 1985; Price, 1987), the radiance can be obtained and hence the bidirectional reflectance factor $R_T(\mu_o, \mu, \varphi)$ at the top of the atmosphere can be derived. The direction of incidence is given by the cosine of the solar zenith angle $\mu_o$ and the direction of observation by the cosine of the zenith angle of observation $\mu$ and the relative azimuth $\varphi$ between the direction of observation and the sun. The directional-hemispherical cloud reflectance $R_c(\mu_o)$ has to be derived from $R_T(\mu_o, \mu, \varphi)$ which is required by the parametrization schemes applied. Using only fully cloudy pixels, which can be identified by the APOLLO scheme (Saunders and Kriebel, 1988), this is possible with additional information on the anisotropy, the atmospheric transmittance above the cloud, the cloud transmission properties, the angular average of $R_c(\mu_o)$ and on the surface albedo underneath the cloud.

The first step is a correction due to the anisotropy of the top-of-atmosphere reflectance which gives the directional-hemispherical reflectance:

$$R_T(\mu_o) = \frac{1}{\pi} \int_0^{2\pi} \int_0^1 R_T(\mu_o, \mu, \varphi)\, \mu \, d\mu \, d\varphi \qquad (1)$$

which is approximated by using anisotropy conversion factors $f(\mu_o, \mu, \varphi)$ computed from Nimbus 7 ERB data (Taylor and Stowe, 1984):

$$R_T(\mu_o) = R_T(\mu_o, \mu, \varphi)/f(\mu_o, \mu, \varphi) \qquad (2)$$

This anisotropy correction is based on global averages of measured radiances and distinguishes only between four cloud-free surfaces and four cloud types. Therefore it does not account for the anisotropy change with increasing optical depth. However, horizontal averaging is presumably the most important source of error if this correction is applied to pixel-size cloudiness. Using NOAA AVHRR channel 1 data (0.58–0.68 $\mu$m) only, water vapour absorption in the clouds and above the clouds can be neglected. However, an ozone correction is required to convert top-of-atmosphere reflectance $R_T(\mu_o)$ to top-of-cloud reflectance $R(\mu_o)$. The ozone transmittance in channel 1, $T_{03}$, has to be applied to both the downwelling and the upwelling radiation which yields

$$\begin{aligned} R(\mu_o) &= R_T(\mu_o)/[T_{03}(\mu_o)\, T_{03}(\overline{\mu, \varphi})] = \\ &= R_T(\mu_o, \mu, \varphi)/[f(\mu_o, \mu, \varphi)\, T_{03}(\mu_o) \cdot \\ &\quad T_{03}(\overline{\mu, \varphi})] \end{aligned} \qquad (3)$$

This top-of-cloud reflectance consists of the cloud reflectance $R_c(\mu_o)$ and of the surface reflectance $A_s$ transmitted through the cloud (e.g. Chandrasekhar, 1950):

$$R(\mu_o) = R_c(\mu_o) + \frac{A_s T_c(\mu_o)\, T_c}{1 - A_s R_c} \qquad (4)$$

Solar irradiance is diffusely transmitted downward through the cloud according to the directional-hemispherical cloud transmittance $T_c(\mu_o)$, illuminates the surface roughly isotropically and is reflected by means of the bihemispherical surface albedo $A_s$. This upwelling radiation is partly reflected downward at the bottom of the cloud according to the bihemispherical cloud reflectance $R_c$ and is partly transmitted through the cloud by means of the bihemispherical cloud transmittance $T_c$ and contributes to the directional-hemispherical reflectance at the top of the cloud, $R(\mu_o)$. The former process is accounted for by the geometric series sum formula. Now we want to replace $A_s$, $T_c(\mu_o)$, $T_c$ and $R_c$ by observable quantities and then to solve Eq. (4) for $R_c(\mu_o)$.

The relationship between the directional-hemispherical and the bihemispherical cloud reflectance can again be obtained from the Nimbus 7 ERB data. In their Figures 8 and 9, Taylor and Stowe (1984) plot the directional-hemispherical reflectance at the top of the atmosphere, $R_T(\mu_o)$, versus the solar zenith angle. The bihemispherical reflectance at the top of the atmosphere, i.e. the angular average of $R_T(\mu_o)$ with respect to $\mu_o$, can be obtained by integrating the plotted directional-hemispherical reflectances:

$$R_T = 2 \int_0^1 R_T(\mu_o)\, \mu_o \, d\mu_o \qquad (5)$$

Using $R_T$, a conversion factor $g(\mu_o)$ can be derived which relates $R_T$ to $R_T(\mu_o)$:

$$R_T = R_T(\mu_o)/g(\mu_o) \tag{6}$$

The assumption is now that the ozone will not alter the anisotropy of the directional-hemispherical reflectance. Then, $g(\mu_o)$ can also be applied to the top-of-cloud reflectances:

$$R = 2\int_0^1 R(\mu_o)\mu_o d\mu_o = R(\mu_o)/g(\mu_o). \tag{7}$$

Because water vapour absorption in clouds is negligible below 0.75 μm (a possible aerosol absorption is neglected), the cloud transmittance can be replaced by 1 – reflectance, i.e. $T_c$ is replaced by $(1 - R_c)$ and $T_c(\mu_o)$ by $(1 - R_c(\mu_o))$. To express $R_c$ in terms of observable quantities, Eq. (4) is integrated with respect to $\mu_o$:

$$\int_0^1 R(\mu_o)\mu_o d\mu_o = \int_0^1 R_c(\mu_o)\mu_o d\mu_o + \\ + \frac{A_s(1-R_c)}{1-A_sR_c}\int_0^1 (1 - R_c(\mu_o))\mu_o d\mu_o \tag{8}$$

The term of the left hand side can be replaced by its angular mean value R/2 which is $R(\mu_o)/2g(\mu_o)$ according to Eq. (7). After rearranging we obtain

$$\frac{R(\mu_o)}{2g(\mu_o)} - \frac{A_s(1-R_c)}{2(1-A_sR_c)} = \\ = \int_0^1 R_c(\mu_o)\mu_o d\mu_o \left(1 - \frac{A_s(1-R_c)}{(1-A_sR_c)}\right) \tag{9}$$

Now $\int_0^1 R_c(\mu_o)\mu_o d\mu_o$ is substituted by its angular mean value $\frac{1}{2}R_c$ and Eq. (9) is then solved for $R_c$:

$$R_c = \frac{R(\mu_o) - g(\mu_o)A_s}{g(\mu_o)(1-2A_s) + R(\mu_o)A_s}. \tag{10}$$

Equation (10) relates the angular mean cloud reflectance to observable quantities. Now Eq. (4) can be solved for $R_c(\mu_o)$ by again replacing $T_c$ and $T_c(\mu_o)$ by $(1 - R_c)$ and $(1 - R_c(\mu_o))$, respectively and substituting $R_c$ by Eq. (10):

$$R_c(\mu_o) = \frac{R(\mu_o)[g(\mu_o)(1-A_s) + A_s] - g(\mu_o)A_s}{g(\mu_o)(1-2A_s) + R(\mu_o)A_s} \tag{11}$$

$R(\mu_o)$ is obtained from Eq. (3), $g(\mu_o)$ from the Taylor and Stowe (1984) data and the surface albedo $A_s$ either from a-priori knowledge deduced from a look-up table derived from previous measurements or from nearest neighbour cloud-free pixels. Fixed values of $A_s$ like 0.1 over land and 0.05 over the ocean should be used only if realistic information cannot be obtained.

## 3 Determination of Cloud Optical Properties

According to Stephens (1978) and Stephens et al. (1984) the directional-hemispherical cloud reflectance $R_c(\mu_o)$ is connected to the cloud optical thickness $\delta$ by

$$R_c(\mu_o) = \frac{\beta(\mu_o)\delta(\mu_o)/\mu_o}{1 + \beta(\mu_o)\delta(\mu_o)/\mu_o} \tag{12}$$

with the modified backscattering coefficient $\beta(\mu_o)$ given for water clouds with optical thicknesses from 1 to 500. From the optical thickness the cloud liquid water path LWP is obtained in $gm^{-2}$ by

$$\log \mathrm{LWP} = (\delta \cdot 0.5454)^{0.254} \tag{13}$$

and the downward and upward infrared emissivity $\epsilon$ by

$$\epsilon\downarrow = 1 - \exp(-0.158\,\mathrm{LWP}) \\ \epsilon\uparrow = 1 - \exp(-0.13\,\mathrm{LWP}) \tag{14}$$

Different formulae have to be applied to ice clouds. According to Platt et al. (1980), ice clouds have a higher reflectance than water clouds for the same optical thickness. The conversion factor depends on $\mu_o$, however no complete data set is given. Therefore at present an average conversion factor of 1.6 is used to reduce the observed ice cloud reflectance to an equivalent water cloud reflectance from which the ice cloud optical thickness is derived according to Eq. (12).

To obtain ice water path and infrared emissivity, a different scheme is used given by Starr and Cox (1985). They relate the broad band albedo $\rho(\vartheta_o)$ to its particular value at the solar zenith angle $\vartheta_o = 60°$:

$$\rho(\vartheta_o) = (0.161 + 0.0117\cdot\vartheta_o + \\ + 0.386\cdot 10^{-4}\cdot\vartheta_o^2)\cdot\rho(60°) + \\ + (0.914 - 0.0152\cdot\vartheta_o)[\rho(60°)]^2 \tag{15}$$

The value at $\vartheta_o = 60°$ is related to the upward infrared emissivity $\epsilon\uparrow$:

$$\rho(60°) = 0.557\cdot\epsilon(\uparrow) + 0.105[\epsilon(\uparrow)]^2 \tag{16}$$

and the emissivity is related to the ice water path IWP:

$$\epsilon(\uparrow,\downarrow) = 1 - \exp[-k(\uparrow,\downarrow)\cdot\mathrm{IWP}] \tag{17}$$

with $k(\uparrow,\downarrow)$ the effective upward and downward broadband infrared mass absorption coefficient in

Table 1 Estimated accuracy of the liquid water path derived from APOLLO.

| Source of error | Estimated amount in % |
|---|---|
| Calibration | ± 10 |
| Anisotropy correction | ± 20 |
| Parametrization scheme | ± 20 |
| Horizontal inhomogeneity | ± 25 |
| Total r.m.s. | ± 40 |

$m^2 g^{-1} \cdot K(\downarrow) = 0.06$ and 0.07 for nighttime and midday, respectively, and $k(\uparrow) = 0.05$. The broadband cloud albedo $\rho(\vartheta_0)$ is lower than the AVHRR channel 1 cloud reflectance $R_c(\vartheta_0)$ by a factor of 1.14 on average. This factor was derived from data given by Welch et al. (1980).

A first estimate shows that the accuracy obtained using this parameterization should not be worsen than ± 50% (Table 1).

## 4 First Validations

Validation of the derived cloud optical properties requires independent measurements of comparable quantities, i.e. of horizontal averages of at least the pixel size. Aircraft measurements seem to be an appropriate means provided the time necessary to obtain horizontal averages does not exceed the time difference allowed between satellite and aircraft measurement which depends on whether it is cumuliform or stratiform cloud. For stratiform cloud the time lag is believed to be less than half an hour, for cumuliform clouds it should be much less. Liquid water content (LWC) can be measured from an aircraft with a Johnson-Williams probe, CSIRO-King probe and Knollenberg PMS-probes. All three have manufacturer's calibration only, with the exception of the PMS-probe where the particle diameter read out can be adjusted. Therefore, additional user performed test procedures are absolutely necessary for obtaining reliable results for all of these probes. Because the results obtained with these devices sometimes do agree and sometimes don't (possibly depending on which drop size dominates), it is questionable which system is superior to the other or what is the real range of uncertainty. From comparisons of many flights and the requirement of consistency with other data, it is believed that the LWC can be measured to an accuracy of ± 30%. This agrees well with results from Strapp and Schemenauer (1982) who demonstrate that under favourable conditions ± 20% can be obtained. To date we have two quasi-simultaneous measurements of the LWP to validate APOLLO derived data with the vertical integral of the liquid water content (LWC) measured with a Johnson-Williams probe by means of the DLR research aircraft DO28. Time resolution of the measurements was better than one second which corresponds to a height resolution of about a metre. These data have been integrated with respect to the vertical extension of the clouds. The assumption is that each airborne LWC measurement represents the horizontal average across the range covered by the slant path. This assumption is valid in homogeneous situations.

Both comparison measurements took place on 19 January 1987 near Manching airport, 48° 42.9'N, 11° 32.1'E (Figure 1). The time difference between the satellite measurement and aircraft measurement was 30–40 minutes. Aircraft navigation is estimated to be much better than the satellite navigation due to the adjacent airport which allowed a precise location. Careful satellite navigation obtains an accuracy of better than a pixel which is less than 1 km. The horizontal projection of the slant path of the aircraft was drawn in the satellite image and the cursor defined a rectangle containing the slant path. The rectangle was set to about 15 by 10 pixels in size to cover the aircraft slant path whicb was around 15 km. The average LWP inside the cursor was determined by means of APOLLO and compared with the vertical integral of the LWC-profile obtained from the aircraft data. In both cases APOLLO yields lower values of the LWP than obtained from the aircraft data (see Table 2).

From Figure 1 it follows that the comparison took place with stratiform clouds with no other clouds above as was also reported from the aircraft. The visual impression of such a situation (Figure 1A) is confirmed by Figure 1B which shows warm temperatures, i.e. low clouds. The high reflectivity in channel 3 (Figure 1C) indicates water clouds (cloud-free snow pixels which could give similar data in Figures 1A and 1B are excluded by means of the snow-ice-cloud discrimination algorithm (Gesell, 1989) which is part of

Table 2 Validation of satellite derived liquid water path (LWP). Percentages indicate the deviation of the APOLLO derived LWP from the aircraft data.

| | Case 1 | Case 2 |
|---|---|---|
| LWP (Aircraft data) in $gm^{-2}$ | 155 | 103 |
| LWP (APOLLO) in $gm^{-2}$ | 95 | 69 |
| $\frac{\Delta LWP}{LWP_{aircraft}}$ in % | 39 | 33 |
| $\frac{\Delta LWP}{LWP_{APOLLO}}$ in % | -63 | -49 |

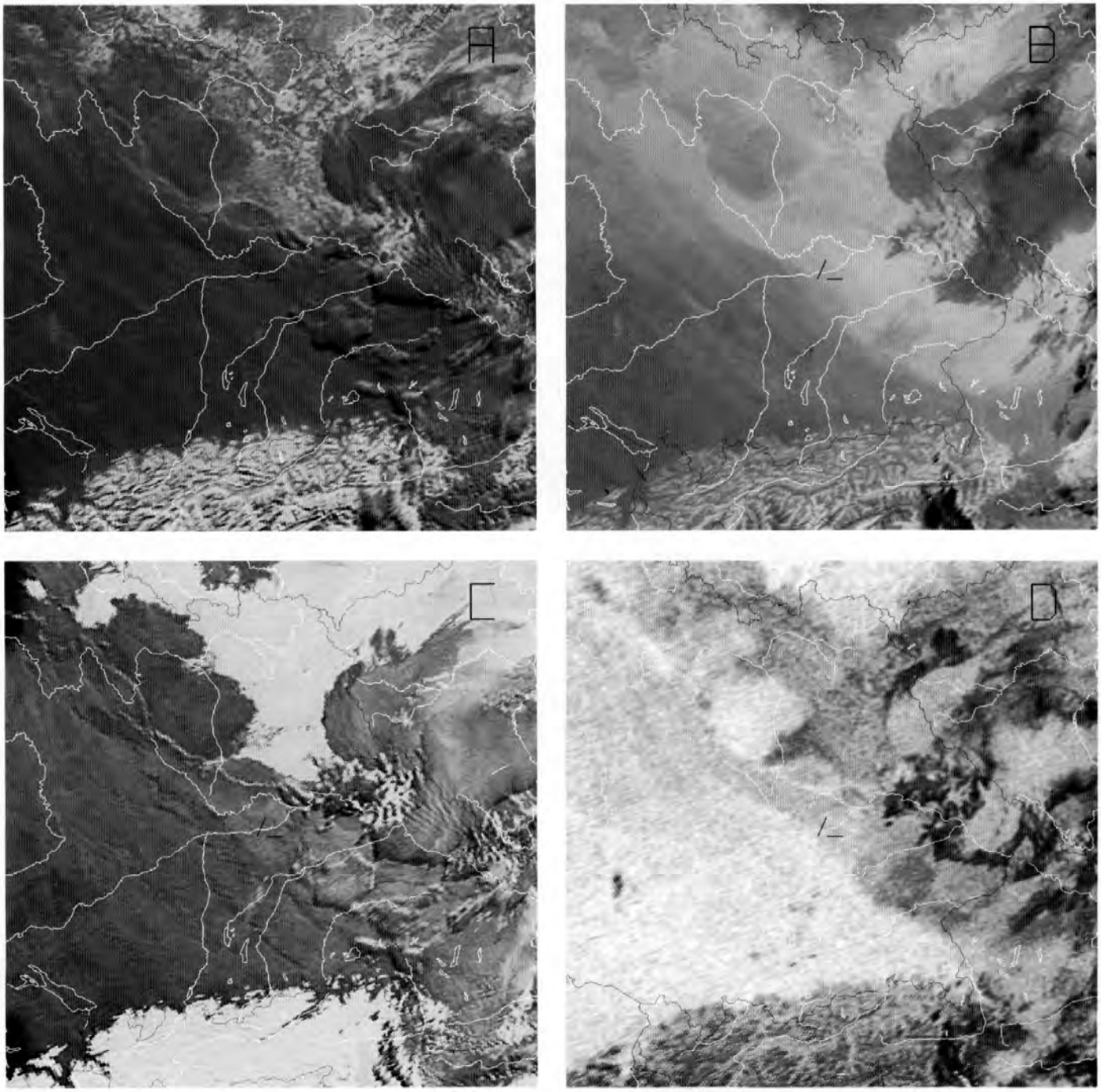


**Figure 1** AVHRR images of the area in which the validation of the APOLLO derived liquid water path data with airborne profiles of the liquid water content took place on 19 January 1987. The horizontal projections of the two aircraft flight legs near Manching airport in Bavaria, FRG, are indicated as the two small straight lines in the center of each figure. In the bottom of each figure the Alps can be seen. Rivers and political boundaries are shown for orientation. The assumption of homogeneous stratiform clouds with no other clouds above, as can be concluded from the visual impression of figure 1A (channel 1) is supported by the three other figures. Figure 1B (channel 4) indicates low clouds, figure 1C (channel 3, reflected radiance only) indicates water clouds, i.e. it is not cloud-free snow, and from figure 1D (channels 4–5) it follows that there was no cirrus on top of the stratus.

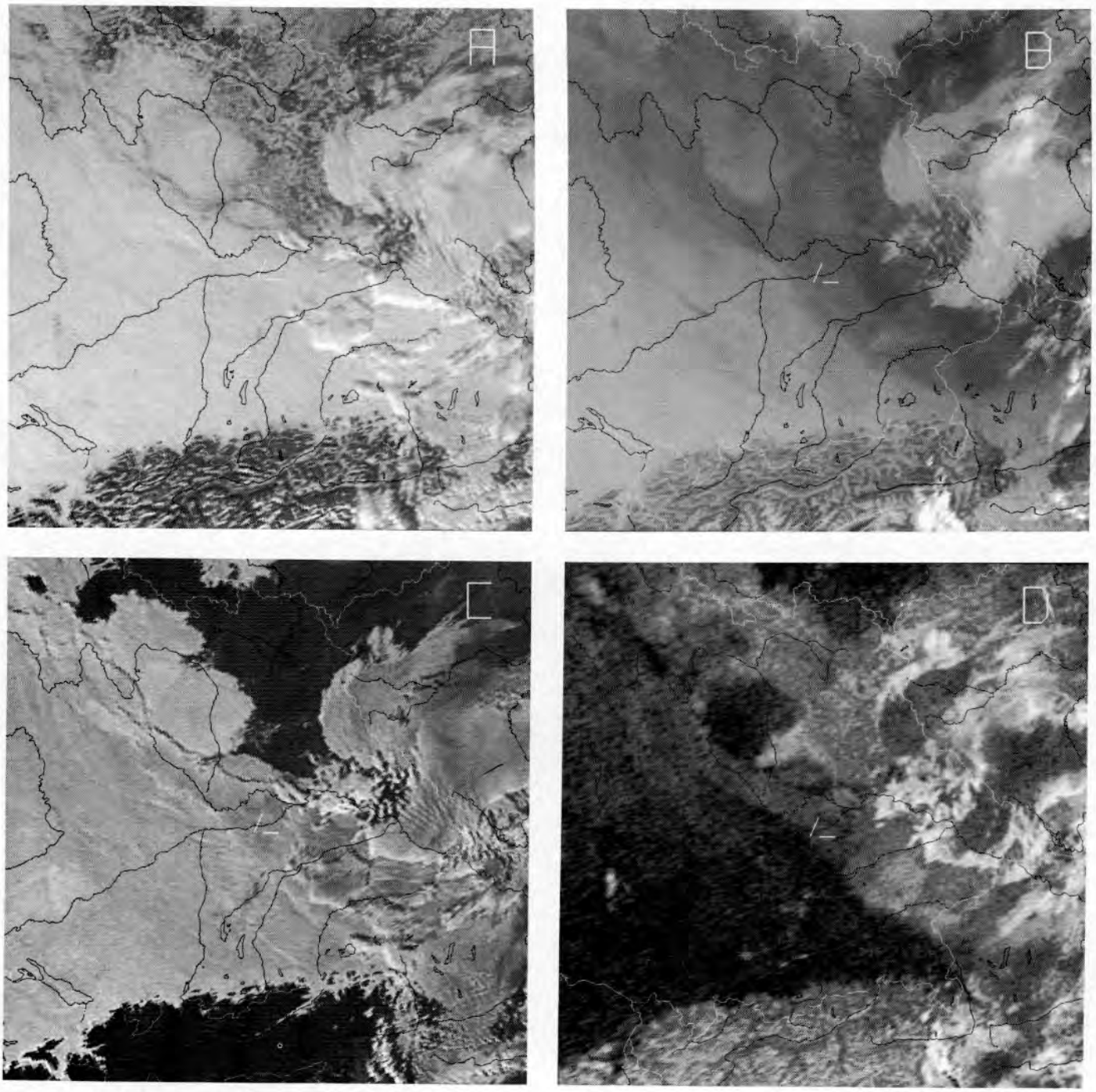


**Figure 1** AVHRR images of the area in which the validation of the APOLLO derived liquid water path data with airborne profiles of the liquid water content took place on 19 January 1987. The horizontal projections of the two aircraft flight legs near Manching airport in Bavaria, FRG, are indicated as the two small straight lines in the center of each figure. In the bottom of each figure the Alps can be seen. Rivers and political boundaries are shown for orientation. The assumption of homogeneous stratiform clouds with no other clouds above, as can be concluded from the visual impression of figure 1A (channel 1) is supported by the three other figures. Figure 1B (channel 4) indicates low clouds, figure 1C (channel 3, reflected radiance only) indicates water clouds, i.e. it is not cloud-free snow, and from figure 1D (channels 4–5) it follows that there was no cirrus on top of the stratus.

APOLLO). Finally, from the low temperature difference between channels 4 and 5 as shown in Figure 1D it follows that no cirrus clouds can be detected above the stratus.

One possible reason for the discrepancy between aircraft and satellite LWP is horizontal inhomogeneity of the LWP as has been thoroughly investigated by Stephens (1988). However, it is not necessary to consider holes in the clouds, i.e. zero LWP, because only cloud filled pixels are used in the APOLLO scheme to derive LWP. A simple calculation shows the order of magnitude of this effect. Assume a pixel whose two halves have a different LWP. The true LWP is the arithmetic mean. AVHRR, however, measures the arithmetic mean of the reflectances produced by the two different LWP's. This mean reflectance is coupled in a different way to the true mean LWP due to the nonlinear relationship between LWP and reflectance (cf. equations 12 and 13). Assuming $\mu_0 = 1$ and $\beta = 0.07$, Table 3 shows the underestimation of the APOLLO derived LWP in terms of a factor by which the APOLLO derived LWP has to be multiplied to obtain the real LWP. This factor depends on the LWP and on the inhomogeneity. Realistic inhomogeneities are less than 3:1 in stratiform clouds (Finger and Wendling, 1990) which is equivalent to a variability of the aircraft measured LWC of ± 50% around its mean value. Curry (1986) reports somewhat higher variabilities close to the cloud top which may reflect the large vertical gradient of the liquid water content above its maximum value. This does not necessarily indicate a higher horizontal variability of the LWP than 3:1. For mixed clouds the inhomogeneity is much higher, however, per kilometer it remains in the 3:1 range (Hoffmann, 1989). This only partly explains the difference between the Johnson-Williams probe and the APOLLO parametrization. It confirms the preliminary estimation of the accuracy of APOLLO which is ± 50% in the LWP.

With cirrus clouds a first validation took place on 1 October 1987 during the first field phase of the International Cirrus Experiment (ICE). This validation compares optical depths of cirrus clouds obtained by APOLLO with airborne lidar measurements obtained from the DLR research aircraft DO228 with the ALEX-F backscattering lidar looking upward. Again the aircraft flight path was drawn in the satellite image and surrounded by a rectangular cursor. The horizontal mean of the optical depth inside the cursor box was estimated to 0.8. The lidar data were processed according to an analytical approach after Klett (Schmitz-Peiffer et al., 1989) and yielded an average optical depth of 0.73. This agreement, however, must be taken only as an indication that the parametrization used in APOLLO for ice clouds is realistic and gives the correct order of magnitude.

**Table 3** Effect of horizontal inhomogeneity of LWP ($\mu_0 = 1$, $\beta = 0.07$)

| Inhomogeneity | Underestimation of LWP by a factor of | | |
|---|---|---|---|
| | LWP > 1000 | 100 < LWP < 1000 | LWP < 100 |
| 9:1 | 2 | 2.33 | 1.61 |
| 3:1 | 1 | 1.25 | 1.11 |
| 1.6:1 | 1 | 1.08 | 1 |

## 5 Conclusions

Parametrized relations between cloud reflectance and cloud optical properties have been applied to satellite data. Emphasis has been put on the derivation of the directional-hemispherical cloud reflectance which is required by the parametrization schemes, from the measured top of the atmosphere reflected radiances. First validations against airborne in-situ measurements indicate agreement within the expected range of uncertainty. Deviations exceed the uncertainty range of the airborne measurements by about ± 25%. Besides the uncertainties connected with the parametrization schemes for homogeneous clouds, this may be due to horizontal inhomogeneities of the cloud composition. To determine the real range of uncertainty, more validations are necessary. Aircraft measurements of the LWP of arctic stratus clouds are presently being investigated to validate simultaneous satellite (NOAA AVHRR) measurements. During ICE 89 more measurements of the cirrus optical depth are expected, probably together with the first measurements of the cirrus ice water path.

## Acknowledgements

The authors are indebted to J. Demmel, H. Fimpel, H. E. Hoffmann, who obtained the airborne LWC data, and to P. Moerl, A. Schmitz-Peiffer, S. Schulz, who obtained the airborne optical depth data, all from DLR, Institut für Physik der Atmosphäre. We gratefully acknowledge the support of the Flight Department Oberpfaffenhofen of DLR.

### References

*Arking, A.* and *J. D. Childs*, 1982: Retrieval of cloud cover parameters from multispectral satellite images. J. Clim. Appl. Meteor. **24**, 322–333.

*Chandrasekhar, S.*, 1950: Radiative Transfer. Oxford Clarendon Press. p. 393.

*Coakley, J. A.* and *P. Chylek*, 1975: The two-stream approximation in Radiative Transfer: Including the angle of the incident radiation. J. Atmos. Sci. **32**, 409–418.

*Curry, J. A.*, 1986: Interactions among Turbulence, Radiation and Microphysics in Arctic Stratus Clouds. J. Atmos. Sci. **43**, 90–106.

*Finger, J. E.* and *P. Wendling*, 1990: Turbulence structure of arctic stratus clouds derived from measurements and calculations. Accepted for J. Atmos. Sci.

*Gesell, G.*, 1989: An algorithm for snow and ice detection using AVHRR data: An extension to the APOLLO software package. Int. J. Remote Sens. **10**, 897–905.

*Hoffmann, H.-E.*, 1989: The horizontal and vertical structures of cloud physical parameters. Extended abstract for conference preprint volume of Fifth WMO Scientific Conference on Weather Modification and Applied Cloud Physics Beijing, China, 8–12 May 1989.

*Kidwell, K. B.*, 1985: NOAA Polar Orbiter Data Users Guide. NOAA/NESDIS, Washington DC.

*Kriebel, K. T.* and *P. Koepke*, 1987: Improvements in the Shortwave Cloud-free Radiation Budget Accuracy. Part II: Experimental Study Including Mixed Surface Albedos. J. Clim. Appl. Meteor., **26**, 396–409.

*Nicodemus, F. E.*, 1970: Reflectance nomenclature and directional reflectance and emissivity. Appl. Optics, 9, 1474–1475.

*Platt, C. M. R.*, *D. W. Reynolds* and *N. L. Abshire*, 1980: Satellite and Lidar observations of the albedo, emittance and optical depth of Cirrus compared to model calculations. Mon. Wea. Rev., **108**, 195–204.

*Price, J. C.*, 1987: Calibration of satellite radiometers and the comparison of vegetation indices. Remote Sens. Environ., **21**, 15–27.

*Rossow, W. B.*, *F. Mosher*, *E. Kinsella*, *A. Arking*, *M. Debois*, *E. F. Harrison*, *P. Minnis*, *E. Ruprecht*, *G. Sèze*, *C. Simmer* and *E. A. Smith*, 1985: ISCCP algorithm intercomparison. J. Clim. Appl. Meteor. **24**, 877–903.

*Saunders, R. W.*, 1986: An automated scheme for the removal of cloud contamination from AVHRR radiances over western Europe. Int. J. Remote Sens., 7, 867–886.

*Saunders, R. W.* and *K. T. Kriebel*, 1988: An improved method for detecting clear sky and cloudy radiances from AVHRR data. Int. J. Remote Sens., 9, 123–150.

*Schmitz-Peiffer, A.*, *W. Renger* and *P. Mörl*, 1989: Fernerkundung von Cirruswolken mit einem flugzeuggetragenen Lidarsystem. Ann. Meteorol. (NF), **26**, 59–60.

*Starr, D. O'C.* and *S. K. Cox*, 1985: Cirrus clouds. Part I: A cirrus cloud model. J. Atmos. Sci. **42**, 2663–2681.

*Stephens, G. L.*, 1978: Radiation profiles in extended water clouds II: Parameterization schemes. J. Atmos. Sci. 35, 2123–2132.

*Stephens, G. L.*, *S. Ackerman* and *E. A. Smith*, 1984: A Shortwave Parameterization Revised to Improve Cloud Absorption. J. Atmos. Sci. **41**, 687–690.

*Stephens, G. L.*, 1988: Radiative Transfer through Arbitrarily Shaped Optical Media. Part I: A General Method of Solution. Part II: Group Theory and Simple Closures. J. Atmos. Sci. 45, 1818–1848.

*Strapp, J. W.* and *R. S. Schemenauer*, 1982: Calibrations of Johnson-Williams Liquid Water Content Meters in a High-Speed Icing Tunnel. J. Appl. Meteor., **21**, 98–108.

*Sundqvist, H.*, *E. Berge* and *J. E. Kristjansson*, 1988: Cloud Parameterisation Studies with a Mesoscale NWP Model. University of Bergen, Section of Meteorology; IBM Bergen Scientific Center, BSC 88/17, Bergen, Norway.

*Taylor, V. R.* and *L. L. Stowe*, 1984: Atlas of reflectance patterns for uniform earth and cloud surfaces (NIMBUS-7 ERB 61 days). NOAA Technical Report NESDIS 10.

*Welch, R. M.*, *S. K. Cox* and *J. M. Davis*, 1980: Solar radiation and clouds. Meteorological Monographs 17, No. 39, May 1980, AMS Ed., Boston, MA, USA, p. 96.